New Phytologist

Uncertainties and limitations of using carbon-13 and oxygen-18 leaf isotope exchange to estimate the temperature response of mesophyll CO_2 conductance in C_3 plants

Balasaheb V. Sonawane and Asaph B. Cousins

School of Biological Sciences, Washington State University, Pullman, WA 99164, USA

Author for correspondence:
Asaph B. Cousins
Tel: +1 509 335 7218
Email: acousins@wsu.edu

Received: *24 May 2018*
Accepted: *28 October 2018*

New Phytologist (2019) **222:** 122–131
doi: 10.1111/nph.15585

Key words: C_3 photosynthesis, carbon isotopes, mesophyll CO_2 conductance, oxygen isotopes, *Panicum bisulcatum*, temperature response.

Summary

- The internal CO_2 gradient imposed by mesophyll conductance (g_m) reduces substrate availability for C_3 photosynthesis. With several assumptions, estimates of g_m can be made from coupled leaf gas exchange with isoflux analysis of carbon $\Delta^{13}C$-g_m and oxygen in CO_2, coupled with transpired water (H_2O) $\Delta^{18}O$-g_m to partition g_m into its biochemical and anatomical components. However, these assumptions require validation under changing leaf temperatures.
- To test these assumptions, we measured and modeled the temperature response (15–40°C) of $\Delta^{13}C$-g_m and $\Delta^{18}O$-g_m along with leaf biochemistry in the C_3 grass *Panicum bisulcatum*, which has naturally low carbonic anhydrase activity.
- Our study suggests that assumptions regarding the extent of isotopic equilibrium (θ) between CO_2 and H_2O at the site of exchange, and that the isotopic composition of the H_2O at the sites of evaporation (δ^{18}_{w-e}) and at the site of exchange (δ^{18}_{w-ce}) are similar, may lead to errors in estimating the $\Delta^{18}O$-g_m temperature response. The input parameters for $\Delta^{13}C$-g_m appear to be less sensitive to temperature. However, this needs to be tested in species with diverse carbonic anhydrase activity.
- Additional information on the temperature dependency of cytosolic and chloroplastic pH may clarify uncertainties used for $\Delta^{18}O$-g_m under changing leaf temperatures.

Introduction

Diffusional limitations to CO_2 movement into and within a leaf result in reduced CO_2 availability at the site of carboxylation and can therefore limit rates of photosynthesis (Evans & von Caemmerer, 1996). The initial resistance to CO_2 diffusion through stomata from the leaf surface (C_a) to the intercellular air spaces (C_i) is well characterized and is known to strongly influence rates of photosynthesis (Warren, 2008). Within a leaf, CO_2 must further diffuse from the intercellular air spaces to the site of carboxylation inside chloroplast for CO_2 fixation by the enzyme Rubisco. These final steps of the CO_2 diffusion pathway are generally referred to as mesophyll CO_2 conductance g_m (Evans & von Caemmerer, 1996).

In C_3 plants, g_m has been shown to vary between species (von Caemmerer & Evans, 2015), to acclimate under different environmental growth conditions (Flexas *et al.*, 2008), and to change with leaf age (Niinemets *et al.*, 2006; Barbour *et al.*, 2016). Additionally, g_m in C_3 plants has been shown to vary in response to short-term changes in measurement temperatures, light, and CO_2 concentration in some but not all species (Flexas *et al.*, 2007; Douthe *et al.*, 2011; Tazoe *et al.*, 2011; Evans & von Caemmerer, 2013; von Caemmerer & Evans, 2015). Leaf properties, such as the arrangement and compactness of mesophyll cells, chloroplast orientation to the intercellular airspaces, and cell wall and membrane properties, have all been proposed to influence adaptive and long-term acclimation of g_m, whereas differences in leaf biochemistry (e.g. carbonic anhydrase (CA) and aquaporins) are thought to potentially drive dynamic g_m responses to short-term changing environments (Gillon & Yakir, 2000; Evans *et al.*, 2009; von Caemmerer & Evans, 2015). However, our understanding of how leaf anatomy and biochemistry influence g_m is incomplete, primarily because there are no direct ways to measure g_m and the contribution of these various components.

Historically, in C_3 plants, combined measurement of g_m using isoflux of carbon (C) in CO_2 ($\Delta^{13}C$-g_m) and isoflux of oxygen (O) in CO_2 and transpired water (H_2O) ($\Delta^{18}O$-g_m) have been used to partition mesophyll conductance into wall conductance g_w (i.e. cell wall, plasma membrane, and cytosol) and chloroplast conductance g_{ch} (i.e. chloroplast membrane and stroma) (Evans *et al.*, 1994; Gillon & Yakir, 2000). Unfortunately, there are several assumptions needed to derive g_m from both the $\Delta^{13}C$-g_m and $\Delta^{18}O$-g_m methods, and only a few studies have simultaneously

combined both methods on a limited number of species (Gillon & Yakir, 2000; Barbour *et al.*, 2016) under a few short-term environmental conditions (irradiance and humidity in cotton; Loucos *et al.*, 2017). Therefore, a critical comparison of the assumptions used to calculate $\Delta^{13}C$-g_m and $\Delta^{18}O$-g_m, particularly in response to temperature, is needed.

For $\Delta^{13}C$-g_m, the Rubisco fractionation factor b is a key variable (Evans *et al.*, 1986). Estimation of b is difficult; consequently, there are only a few reports on b, and uncertainties remain in its temperature dependency (O'Leary *et al.*, 1992; Tcherkez & Farquhar, 2005; Evans & von Caemmerer, 2013). In addition, in the absence of a species-specific temperature response of the CO_2 compensation point at the site of carboxylation (Γ^*) and gas-exchange measurements at 2% [O_2], there could be potential uncertainties for the temperature dependency of fractionation factors associated with respiration and photorespiration, respectively (Evans & von Caemmerer, 2013).

Alternatively, for the $\Delta^{18}O$-g_m calculations, it is unclear if the CO_2 and the H_2O at the site of exchange are in full isotopic equilibrium θ and if the isotopic signature of the H_2O at the site of evaporation δ^{18}_{w-e} accurately represents the H_2O signature at the site of exchange δ^{18}_{w-ce}. The assumption that there is a full isotopic equilibrium between CO_2 and H_2O at the site of exchange (e.g. $\theta = 1$) is primarily estimated by the activity of leaf CA. However, published CA activity varies widely between studies, species, tissue collection methods, and growth conditions (Hatch & Burnell, 1990; Gillon & Yakir, 2000; Cousins *et al.*, 2008). Boyd *et al.* (2015) suggested deactivation of CA activity in *Setaria viridis* at temperatures above 25°C. In addition, the influence of temperature-induced changes in pH on CA activity cannot be ruled out. Therefore, changes in leaf temperature may offset θ from 1, and this may be higher in species with low CA activity, particularly above 25°C. The assumption that the $\delta^{18}_{w-ce} = \delta^{18}_{w-e}$ has been justified because the distance between the outer cell wall and the chloroplast appressed to the intercellular airspace is short and may lead to the only small gradient in $H_2{}^{18}O$ enrichment (Gillon & Yakir, 2000; Barbour *et al.*, 2016). However, changing leaf temperatures may change H_2O flux inside the leaf and potentially the location that H_2O transitions between the liquid and vapor phase (Buckley *et al.*, 2017). Taken together, assumptions regarding parameter values in calculations of $\Delta^{13}C$-g_m and $\Delta^{18}O$-g_m may propagate uncertainties in estimating g_m in C_3 plants as leaf temperature changes.

Assuming that the calculations of $\Delta^{13}C$-g_m and $\Delta^{18}O$-g_m are parameterized correctly, it has been suggested that $\Delta^{13}C$-g_m provides estimates of the total mesophyll conductance from the intercellular air spaces to the chloroplast stroma, whereas $\Delta^{18}O$-g_m estimates internal CO_2 conductance to the chloroplast surface (Gillon & Yakir, 2000; Barbour *et al.*, 2016). Accordingly, the $\Delta^{13}C$-g_m is often expected to be *c.* $0.66 \times \Delta^{18}O$-g_m (Yakir, 1998). However, short-term changes in leaf temperatures affect the rate of diffusional processes and biochemical reactions; hence, temperature affects CO_2 diffusion through membranes and liquid path, H_2O fluxes, and CO_2–H_2O equilibrium within a leaf (Evans & von Caemmerer, 2013; Barbour *et al.*, 2016). Therefore, investigating temperature dependency of $\Delta^{18}O$-g_m coupled with the $\Delta^{13}C$-g_m provides an opportunity to test the assumptions associated with estimating $\Delta^{13}C$-g_m and $\Delta^{18}O$-g_m.

Here, we simultaneously determined the temperature response of $\Delta^{13}C$-g_m and $\Delta^{18}O$-g_m to test the assumptions used for $\Delta^{13}C$-g_m against $\Delta^{18}O$-g_m, and vice versa. For this, we measured photosynthetic $\Delta^{13}C$ and $\Delta^{18}O$ under changing leaf temperatures, leaf CA activities, and the pH response of CA activity. We used the C_3 grass *Panicum bisulcatum*, which has high rates of CO_2 assimilation and stomatal conductance but naturally low CA activity. Comparison of the temperature responses of $\Delta^{13}C$-g_m and $\Delta^{18}O$-g_m suggests that errors in assumptions of parameters in $\Delta^{18}O$-g_m calculations will strongly influence g_m estimates. By contrast, calculations of $\Delta^{13}C$-g_m appeared to be more temperature robust.

Materials and Methods

Plant material and growth environment

Panicum bisulcatum (PI286485) seeds were germinated in a commercial Sun Gro® Sunshine® LC1 Grower Mix with RESiLIENCE™ (http://www.bfgsupply.com) at the Washington State University, Pullman, WA, USA, in a controlled-environment growth cabinet (model GC-16; Enconair Ecological Chambers Inc., Winnipeg, MB, Canada). Growth conditions were set at 16 h photoperiod including a 2 h ramp at the beginning and at the end of the light period and maximum photosynthetic photon flux density of 600 μmol m^{-2} s^{-1}. Light and dark temperatures were maintained at 28 ± 1 and 18 ± 1°C, respectively, and the mean relative humidity was 60 ± 7%. At 2–3 wk after germination, two healthy seedlings were transplanted into a 2 l pre-irrigated pot containing grower mix used for the germination. A week later, one seedling was removed, leaving one healthy plant per pot. Subsequently, plants were watered daily to field capacity for the remainder of the experiment and received 21-5-20 fertilizer (JR Peters Inc., Allentown, PA, USA; http://www.jrpeters.com) with Scott-Peters Soluble Trace Element Mix (The Scotts Co., Marysville, OH, USA) twice a week at concentrations in H_2O of 2.5 g l^{-1} and 10.0 mg l^{-1}, respectively. Plant location within the growth chamber was randomized daily.

Coupled leaf gas exchange and isoflux measurements

The LI-6400XT infrared gas analyzer (Li-Cor, Lincoln, NE, USA; operating as an open system), cavity-ring down absorption spectroscope (L2130-i; Picarro Inc., Sunnyvale, CA, USA), and the tunable-diode laser absorption spectroscope (TDLAS, model TGA 220A; Campbell Scientific Inc., Logan, UT, USA) were coupled as described by Ubierna *et al.* (2017). The entire LI-6400XT, the 2 cm × 6 cm leaf chamber (6400-11, Li-Cor), and LI-6400-18-RGB light source were placed in a growth cabinet (model EF7, Conviron; Controlled Environments Inc., MN, USA). The inlet gas line to the LI-6400XT cuvette was split using a brass Tee (Swagelok® Tube Fitting, http://www.swagelok.com) and part of the flow was diverted to the TDLAS (reference gas). The flow from the matching tube of the LI-6400XT leaf sample cuvette (sample gas) was split between the L2130-i and the

TDLAS. Air supplied to the TDLAS was passed through a Nafion® dryer (PD™-200T-12; Perma Pure LLC, Toms River, NJ, USA), and the sample line tube (type 1300 Synflex®) for the L2130-i was wrapped with an electrical heating cable to avoid condensation (Kolbe & Cousins, 2018).

The TDLAS data were calibrated using the concentration series method (Tazoe *et al.*, 2011, Supporting Information 1; Ubierna *et al.*, 2013), and the TDLAS levels of precision (standard deviation) for CO_2 ($^{12}CO_2$ + $^{13}CO_2$) molar fraction, $\delta^{13}C$, and $\delta^{18}O$ were ± 0.06 μmol CO_2 mol^{-1} dry air, ± 0.26‰, and ± 0.21‰, respectively. It should be noted that the $\delta^{18}O$ signature was expressed to a common scale (Vienna standard mean ocean water) for comparison of absolute values with the L2130-i.

The L2130-i was calibrated using three running standards calibrated against standard light Antarctic precipitation and Puerto Rico (US Geological Survey) standards. To correct for the concentration dependency of the L2130-i measurements, a standard curve of H_2O vapor concentration ([H_2O]; ppm) of a known and constant δ^{18}_w was determined (Supporting Information Fig. S1a). Corrections were made for all measurements at or above 20 000 ppm (Fig. S1b). The L2130-i precision (standard deviation) for δ^{18}_w of H_2O vapor was ± 0.44‰.

$\Delta^{13}C$ and $\Delta^{18}O$ (the leaf C and O isotope net discrimination of CO_2, respectively) and δ^{18}_{w-out} (the $\delta^{18}O$ of H_2O vapor leaving the leaf chamber) were measured at leaf temperatures of 15, 20, 25, 30, 35, and 40°C on the youngest fully expanded leaf from four plants placed in the LI-6400XT leaf chamber. All measurements started at either 25 or 30°C, and the subsequent measurement temperatures were randomly selected and controlled using both the growth cabinet and LI-6400XT temperature control systems. Throughout the measurements, the desiccant and the soda lime column of the LI-6400XT were fully bypassed. The inlet gas to the LI-6400XT was CO_2 and H_2O free, and no supplemental H_2O vapor was added to the reference gas. Therefore, the concentration and isotopic composition of H_2O vapor leaving the chamber was only determined by leaf transpiration. The leaf chamber was maintained at a CO_2 partial pressure of $C_a \approx 35$ Pa, 2% [O_2] and a photosynthetic photon flux density of 1200 μmol m^{-2} s^{-1}. To avoid errors associated with [O_2] in the gas-exchange calculations, the LI-6400XT program was edited for 2% O_2. Every day, before the leaf measurements, a leak test was determined on an empty LI-6400XT chamber at $C_a \approx 20$ Pa. At each measurement temperature the leaves were acclimated for minimum 30 min or until stable values of A_{net} and g_s were achieved. Data were subsequently collected over the next 20 min and the LI-6400XT was set to log data only when the TDLAS analyzed the sample line.

Leaf C isotope discrimination ($\Delta^{13}C$) and leaf O isotope discrimination ($\Delta^{18}O$)

We use δ^{13} and δ^{18} for $\delta^{13}C$ and $\delta^{18}O$ values of CO_2, respectively, and the $\delta^{18}O$ in H_2O vapor or liquid H_2O is referred to as δ^{18}_w. The observed photosynthetic discrimination against $^{13}CO_2$ ($\Delta^{13}C$) and $C^{18}O^{16}O$ ($\Delta^{18}O$) was calculated as (Evans *et al.*, 1986):

$$\Delta = \frac{\frac{C_{in}}{C_{in}-C_{out}}(\delta_{out}-\delta_{in})}{1+\delta_{out}-\frac{C_{in}}{C_{in}-C_{out}}(\delta_{out}-\delta_{in})} \quad \text{Eqn 1}$$

(C is the $^{12}CO_2$ mole fraction in dry air in and out of the leaf chamber; δ refers to either the $\delta^{13}C$ or the $\delta^{18}O$ in the calculation of $\Delta^{13}C$ or $\Delta^{18}O$, respectively).

CO_2 mesophyll conductance from $\Delta^{13}C$ ($\Delta^{13}C$-g_m)

$\Delta^{13}C$-g_m was calculated from the difference between estimated C isotope discrimination for C_3 plants assuming infinite g_m (Δ^{13}_i), and that measured by the LI6400XT and TDLAS coupled system (Farquhar & Cernusak, 2012):

$$\Delta^{13}_i = \frac{1}{1-t}\left(a_b\frac{C_a-C_s}{C_a}+a_s\frac{C_s-C_i}{C_a}\right) + \frac{1+t}{1-t}\left(b\frac{C_i}{C_a}-e\prime\frac{\alpha_b}{\alpha_{e\prime}}\frac{R_d}{A_{net}+R_d}\frac{C_i-\Gamma^*}{C_a}-f\frac{\alpha_b}{\alpha_f}\frac{\Gamma^*}{C_a}\right) \quad \text{Eqn 2}$$

The definition and derivation of variables are explained in Table S1. The CO_2 compensation point at the site of carboxylation, Γ^* and its temperature dependency in *P. bisulcatum* was estimated according to Sharwood *et al.* (2016).

The difference between Δ^{13}_i and $\Delta^{13}C$ provides mesophyll resistance r_m by (Farquhar & Cernusak, 2012):

$$r_m = \frac{1-t}{1+t}(\Delta^{13}_i-\Delta^{13}C)\frac{C_a}{A\left(b-a_m-\frac{\alpha_b}{\alpha_e}e\prime\frac{R_d}{A_{net}+R_d}\right)} \quad \text{Eqn 3}$$

(a_m is the fractionation during diffusion and dissolution of CO_2 through the H_2O). Note that Eqn 3 is presented in Farquhar & Cernusak (2012, Appendix 3) and used by Barbour *et al.* (2016).

It can be written as:

$$\Delta^{13}C\text{-}g_m = \frac{1}{r_m} \quad \text{Eqn 4}$$

According to Fick's law of diffusion, the leaf mesophyll [CO_2] by the ^{13}C method was derived as:

$$C_{c13} = C_i - \frac{A_{net}}{\Delta^{13}C\text{-}g_m} \quad \text{Eqn 5}$$

(C_{c13} is chloroplastic [CO_2] estimated by $\Delta^{13}C$-g_m).

CO_2 mesophyll conductance from $\Delta^{18}O$ ($\Delta^{18}O$-g_m)

Calculation of mesophyll conductance from $\Delta^{18}O$ ($\Delta^{18}O$-g_m)

The $\delta^{18}O$ of H_2O vapor transpired by the leaf (δ^{18}_{w-E}) is given by

(Simonin *et al.*, 2013):

$$\delta^{18}_{w-E} = \frac{W_{out}\delta^{18}_{w-out} - W_{in}\delta^{18}_{w-in} + \frac{(\delta^{18}_{w-in} - \delta^{18}_{w-out})W_{out}W_{in}}{1000}}{W_{out} - W_{in}} \quad \text{Eqn 6}$$

where δ^{18}_{w-in} and δ^{18}_{w-out} are the $\delta^{18}O$ of H_2O vapor entering (W_{in}) and leaving (W_{out}) the leaf chamber, respectively. In the current study, dry air was used for the inlet air, so $\delta^{18}_{w-E} = \delta^{18}_{w-out}$. The $\delta^{18}O$ of liquid H_2O at the sites of evaporation within the leaf was calculated with the modified Craig–Gordon model (Bottinga and Craig, 1968):

$$\delta^{18}_{w-e} = \delta^{18}_{w-E} + \varepsilon^* + \varepsilon_k + (\delta^{18}_{w-out} - \varepsilon_k - \delta^{18}_{w-E})\frac{e_a}{e_i} \quad \text{Eqn 7}$$

where ε^* is the equilibrium fractionation during H_2O evaporation from liquid to vapor and it is temperature (T_k) dependent, given as (Bottinga and Craig, 1968):

$$\varepsilon^* = 2.664 - 3.206\left(\frac{1000}{T_k}\right) + 1.534\left(\frac{10^6}{T_k^2}\right) \quad \text{Eqn 8}$$

The ε_k is the kinetic fractionation of $H_2{}^{18}O$ diffusion from the leaf intercellular airspace to the atmosphere, which is dependent on boundary layer g_b and stomatal g_s conductance and their associated fractionation factors (Farquhar *et al.*, 1989):

$$\varepsilon_k = \frac{28g_s^{-1} + 19g_b^{-1}}{g_s^{-1} - g_b^{-1}} \quad \text{Eqn 9}$$

The $\delta^{18}O$ of CO_2 at the sites of exchange in the cytosolic δ^{18}_{ce}, assuming that H_2O at the site of exchange δ^{18}_{w-ce} is isotopically the same as H_2O at the sites of evaporation δ^{18}_{w-e}, was calculated as (Cernusak *et al.*, 2004):

$$\delta^{18}_{ce} = \delta^{18}_{w-e}\theta(1 + \varepsilon_w) + \theta\varepsilon_w + \delta_{c0}(1 - \theta) \quad \text{Eqn 10}$$

where δ_{c0} is the $\delta^{18}O$ of unreacted CO_2, θ is isotopic equilibrium between CO_2 and H_2O, and ε_w is the temperature T_k equilibrium fractionation between chloroplast CO_2 and H_2O given as:

$$\varepsilon_w = \frac{17604}{T_k} - 17.93 \quad \text{Eqn 11}$$

The leaf mesophyll [CO_2] can be calculated with the ^{18}O method (C_{m18}) solving Eqn S4 and Eqn 10 for C_{m18} and assuming complete isotopic equilibrium ($\theta = 1$), where δ^{18}_{ce} equals the $\delta^{18}O$ of cytosolic CO_2 δ^{18}_c, as (Barbour *et al.*, 2016; Ubierna *et al.*, 2017):

$$C_{m18} = \frac{C_i(\delta^{18}_i - \alpha^{18}_w\delta^{18}_A - a^{18}_w)}{\delta^{18}_{ce} - \alpha^{18}_w\delta^{18}_A - a^{18}_w} \quad \text{Eqn 12}$$

where the definition and derivation of variables are explained in Methods S1 and Table S2.

According to Fick's law of diffusion:

$$\Delta^{18}O\text{-}g_m = \frac{A_{net}}{C_i - C_{m18}} \quad \text{Eqn 13}$$

Modeling temperature response of Rubisco discrimination factor *b*, isotopic equilibrium θ, and $\delta^{18}O$ of H_2O at the sites of evaporation (δ^{18}_{w-e})

The estimation of $\Delta^{13}C$-g_m in Eqn 2 assumes that the Rubisco fractionation factor b is independent of the temperature. Similarly, the estimation of $\Delta^{18}O$-g_m assumes that the local cytosolic H_2O δ^{18}_{w-ce} is isotopically similar to the H_2O at the sites of evaporation δ^{18}_{w-e} (Eqn 10) and that there is a full equilibrium between CO_2 and cytosolic H_2O ($\theta = 1$). We tested these assumptions, with the caveat that $\Delta^{18}O$-g_m measures g_m to the chloroplast surface and that $\Delta^{13}C$-g_m estimates g_m to the site of carboxylation, such that the inherent difference between $\Delta^{13}C$-g_m and $\Delta^{18}O$-g_m is primarily determined by the conductance across the chloroplast envelope and can be accounted for as $\Delta^{13}C$-$g_m \approx 0.66 \times \Delta^{18}O$-$g_m$ across temperatures. For simplicity across the leaf temperatures, we derived the optimal solution needed to minimize the residual sum of squares for b, θ, and δ^{18}_{w-e} assuming that the $\Delta^{13}C$-g_m is equal to the $\Delta^{18}O$-g_m, and vice versa.

Leaf CA activity and pH response

Fresh leaf discs (0.71 cm^2) were extracted on ice in a mortar with a pestle in 1 ml of 100 mM HEPES (pH 7.8), 1% (w/v) polyvinylpolypyrrolidone, 1 mM EDTA, 10 mM dithiothreitol, 0.1% (v/v) Triton X-100, and 2% (v/v) protease inhibitor cocktail (P9599; Sigma-Aldrich). Crude extracts were centrifuged at 4°C for 1 min at 17 000 ***g***, and the supernatant was collected for immediate use in the CA assay. CA activity was measured using a membrane inlet mass spectrometer to measure the rates of $^{18}O_2$ exchange from labeled $^{13}C^{18}O_2$ to $H_2{}^{16}O$ with a total C concentration of 1 mM (Silverman, 1982; Badger and Price, 1989; Hatch & Burnell, 1990). The pH response of hydration rates k_{CA} was calculated from the enhancement in the rate of ^{18}O loss over the uncatalyzed rate with the nonenzymatic first-order rate constant for the hydration of CO_2 calculated for the assay pH (6.8–8.2) at 25°C using the equation from (Jenkins, 1989). The CO_2 concentration was calculated using the temperature-appropriate pK_a assuming an ionic strength of 0.1 M (Harned & Bonner, 1945), and the pCO_2 was calculated using the temperature-appropriate Henry's constant (Sander, 2015). The temperature dependency of leaf CA activity CA_{leaf} was estimated at pH 8.0 using our measured temperature response of $\Delta^{13}C$-g_m to derive chloroplast [CO_2] and the temperature dependency of CA activity according to Boyd *et al.* (2015). The pH sensitivity of leaf CA was predicted using our measured pH response of k_{CA}, $\Delta^{13}C$-g_m-derived chloroplast [CO_2] and the temperature dependency of CA of Boyd *et al.* (2015).

Statistical analysis

Statistical analyses and estimation of the optimal solution for parameters were performed using R (R Core Team, 2017). The effect of temperature was compared using a linear mixed-effect model using the LME4 package (Bates *et al.*, 2015). Significance tests were performed using ANOVA ($n = 4$). Variable means were ranked using a *post hoc* Tukey test.

Results

Temperature response of gas exchange and discrimination

The rate of net CO_2 assimilation A_{net} was responsive to changes in leaf temperature from 15 to 35°C, with temperature optimum around 35°C (Fig. 1a; Table S3). Similarly, stomatal conductance g_s increased with leaf temperature from 15 to 30°C, but was unchanged above 30°C, despite increases in the leaf-to-air vapor pressure deficit at 35 and 40°C (Fig. 1b,c; Table S3). The ratio of intercellular to ambient [CO_2] C_i/C_a did not significantly change across measurement temperatures ($P > 0.05$; Fig. 1d; Table S3); however, the transpiration rates E increased significantly ($P < 0.05$) with temperature (Fig. S2). In general, the C isotope discrimination $\Delta^{13}C$ tended to increase with temperature, except at 15°C where $\Delta^{13}C$ was similar to the 30 and 35°C values (Fig. 1e; Table S3). Conversely, the O isotope discrimination $\Delta^{18}O$ decreased with temperature, except at 40°C compared with 35°C (Fig. 1f; Table S3).

Comparison of $\Delta^{13}C$-g_m and $\Delta^{18}O$-g_m

The mesophyll conductance derived from $\Delta^{13}C$ $\Delta^{13}C$-g_m, assuming a constant Rubisco discrimination factor b of 29‰, increased significantly with leaf temperature ($P_{5,14} < 0.001$). However, the mesophyll conductance derived from $\Delta^{18}O$ $\Delta^{18}O$-g_m, assuming fully isotopic equilibrium of CO_2 with the H_2O at the site of evaporation, increased with temperature between 15 and 30°C but did not respond from 30 to 40°C (Fig. 2; Table S3). As already described, the $\Delta^{13}C$-g_m and $\Delta^{18}O$-g_m estimated did not differ between 15 and 25°C;

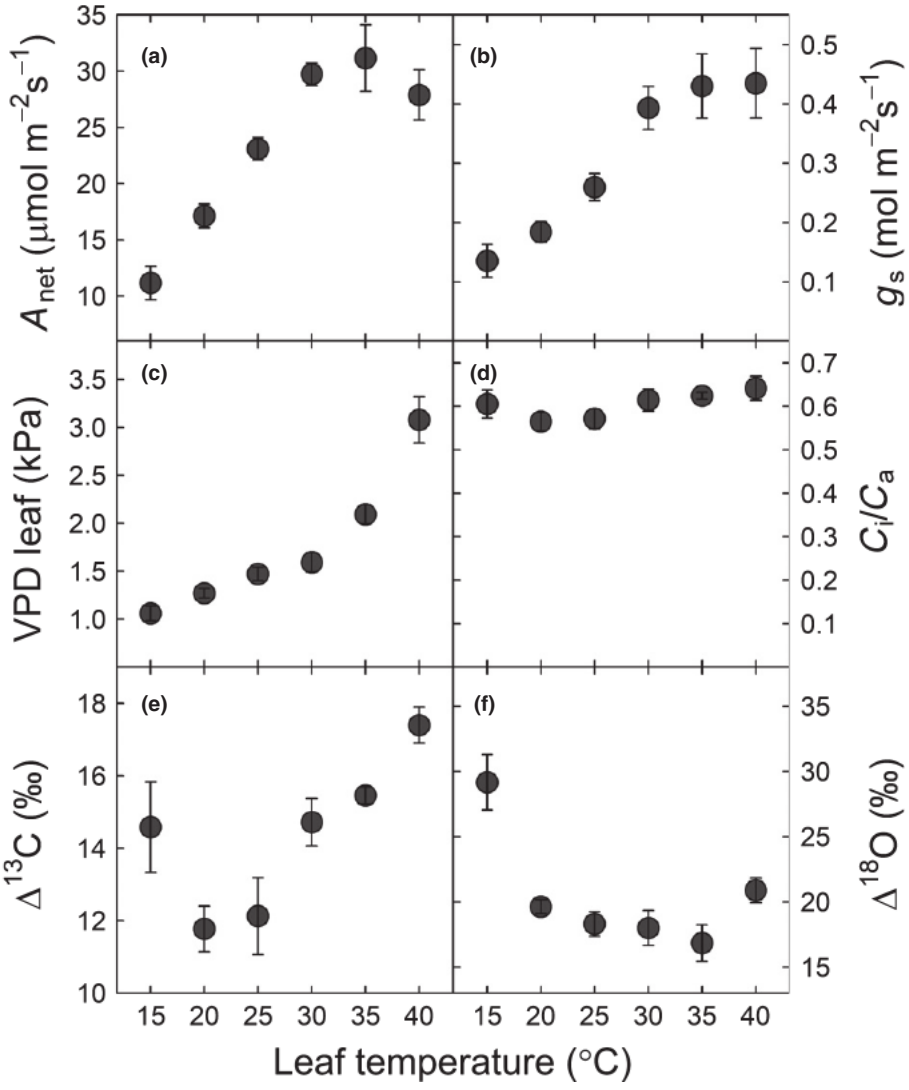

Fig. 1 The temperature response of (a) the net rate of CO_2 assimilation (A_{net}), (b) stomatal conductance to water (g_s), (c) leaf-to-air vapor pressure deficit (VPD leaf), (d) ratio of intercellular to ambient [CO_2] C_i/C_a, (e) leaf carbon isotope discrimination ($\Delta^{13}C$), and (f) leaf oxygen isotope discrimination ($\Delta^{18}O$) in *Panicum bisulcatum*. Measurements were performed at *c.* 35 Pa [CO_2], 1200 μmol m^{-2} s^{-1} photosynthetic photon flux density and 2% [O_2]. Values are mean ± SE, $n = 4$.

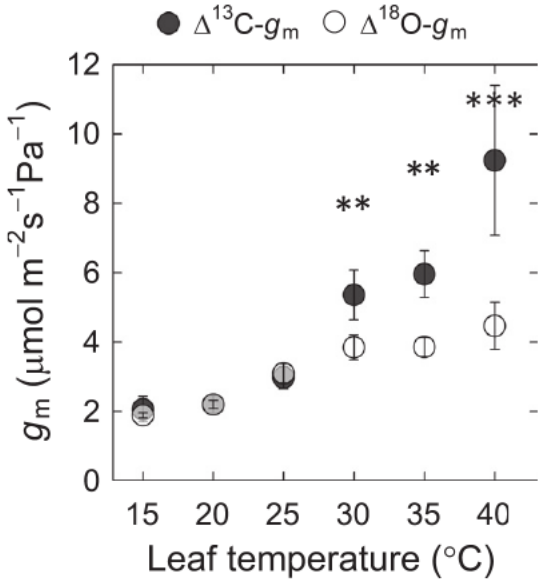

Fig. 2 The temperature response of mesophyll conductance (g_m), calculated with $\Delta^{13}C$-g_m method assuming Rubisco fractionation factor $b = 29‰$ for all temperatures (closed circles) and $\Delta^{18}O$-g_m method (open circles) in *Panicum bisulcatum*. For $\Delta^{18}O$-g_m method, g_m was calculated assuming isotopic equilibrium ($\theta = 1$) and $\delta^{18}_{w-e} = \delta^{18}_{w-ce}$. Repeated measures ANOVA and pairwise comparisons between two methods across leaf temperature were used to test statistical significances: **, $P < 0.01$; ***, $P < 0.001$. Values are mean ± SE, $n = 4$.

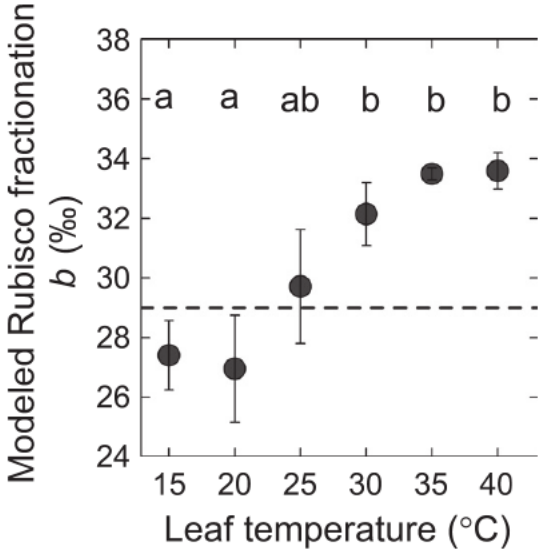

Fig. 3 Modeled changes in Rubisco fractionation factor *b* needed to minimize the difference between the $\Delta^{13}C$-g_m and the measured $\Delta^{18}O$-g_m in *Panicum bisulcatum*. Dashed line represents $b = 29‰$ used in estimating $\Delta^{13}C$-g_m in Fig. 2. The letters are ranking (from lowest = a) for temperatures derived using a multiple-comparison Tukey *post hoc* test. Values are mean ± SE, $n = 3$.

however, between 30 and 40°C the $\Delta^{13}C$-g_m was significantly higher than the $\Delta^{18}O$-g_m (Fig. 2; Table S3), suggesting uncertainty in the assumptions made for $\Delta^{13}C$-g_m and $\Delta^{18}O$-g_m across the measurement temperatures.

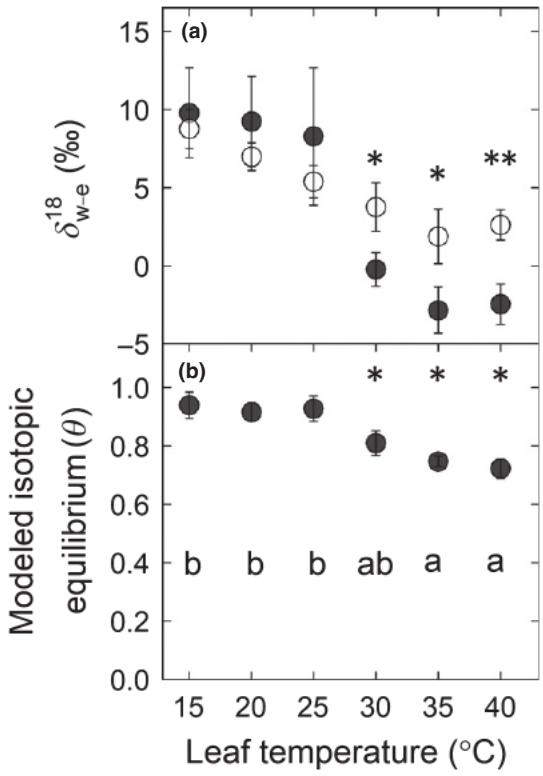

Fig. 4 The temperature response of measured $\delta^{18}O$ of the liquid water at the sites of evaporation inside the leaf δ^{18}_{w-e} (open circles) and modeled δ^{18}_{w-e} (closed circles) needed to minimize the difference between $\Delta^{18}O$-g_m and $\Delta^{13}C$-g_m in *Panicum bisulcatum* (a). Asterisks in (a) represent significance for pairwise comparison between two methods across leaf temperatures. The temperature response of modeled isotopic equilibrium (θ) assuming $\Delta^{18}O$-g_m is equal to $\Delta^{13}C$-g_m in *P. bisulcatum* (b). Asterisks in (b) represent significance for one sample *t*-test across leaf temperatures indicating measured value is statistically different from 1. The letters are ranking (from lowest = a) for temperatures derived using a multiple-comparison Tukey *post hoc* test. Values are mean ± SE, $n = 4$. *, $P < 0.05$; **, $P < 0.01$.

Temperature response of Rubisco discrimination factor *b*, $\delta^{18}O$ of H_2O at the sites of evaporation δ^{18}_{w-e}, and isotopic equilibrium θ

As already described, $\Delta^{13}C$-g_m was initially estimated with a constant *b* across temperatures. Therefore, the *b* value was numerically solved for to minimize the difference between $\Delta^{13}C$-g_m and $\Delta^{18}O$-g_m at each measurement temperature, resulting in a significant change in *b* with temperature ($P_{5,10} < 0.01$) from 27.4 ± 1.2 to $33.6 \pm 0.6‰$ (Fig. 3). Alternatively, the $\Delta^{18}O$-g_m presented in Fig. 2 is based on the assumption that CO_2 is fully equilibrated (i.e. $\theta = 1$) with H_2O at the sites of exchange. The O isotope signature of transpired H_2O δ^{18}_{w-E} did not change significantly with temperature (Fig. S3) but the isotopic signature of H_2O at the site of evaporation δ^{18}_{w-e} significantly decreased with temperature (Fig. 4a).

Therefore, the difference between $\Delta^{13}C$-g_m and $\Delta^{18}O$-g_m could also be explained by errors in parameterizing the $\delta^{18}O$ of H_2O at the sites of evaporation (δ^{18}_{w-e}. For example, assuming that *b* is constant at 29‰ for $\Delta^{13}C$-g_m and $\theta = 1$ across

temperatures then the δ^{18}_{w-e} needed to minimize the difference between $\Delta^{18}O$-g_m and $\Delta^{13}C$-g_m resulted in significantly lower values at leaf temperatures ≥ 30°C (Fig. 4a). Alternatively, assuming that b is constant at 29‰ for $\Delta^{13}C$-g_m and δ^{18}_{w-e} is correct then θ can be solved for to minimize differences between $\Delta^{18}O$-g_m and $\Delta^{13}C$-g_m across leaf temperatures. This caused θ to significantly differ from one at leaf temperature ≥ 30°C ($P_{5, 14} < 0.001$) (Fig. 4b).

pH sensitivity of CA activity at chloroplastic [CO_2]

The pH sensitivity of k_{CA} from pH 6.8 to 8.2 measured with the membrane inlet mass spectrometer showed an exponential increase with pH: $k_{CA} = 5 \times 10^{-8}\, e^{2.1019 \times pH}$ (Fig. 5). At > 25°C the CA_{leaf}, derived using the k_{CA} at pH 8.0 and C_{c13}, increased with temperature (Fig. 6). This assumes pH remains constant with temperature; however, a shift in pH with temperature would have a significant influence on CA_{leaf}. For example, across all temperatures the modeled CA_{leaf} was significantly lower at pH 7.8 and significantly higher at pH 8.2 compared with pH 8.0 (Fig. 6; dashed vs dotted lines, respectively).

Discussion

Temperature dependency of $\Delta^{13}C$-g_m and $\Delta^{18}O$-g_m

In the current study, net CO_2 assimilation A_{net}, stomatal conductance g_s, and $\Delta^{13}C$-g_m in *P. bisulcatum* increased with leaf temperature, similar to that reported by von Caemmerer & Evans (2015) for a large number of C_3 species. The short-term temperature response of $\Delta^{13}C$-g_m has been attributed to changes in CO_2 diffusion through the liquid phase (including cell wall, cytoplasm, and chloroplast stroma) and the membrane phase (including the plasma membrane and chloroplast envelopes) (Evans & von Caemmerer, 2013; von Caemmerer & Evans, 2015). However, precise quantification of $\Delta^{13}C$-g_m depends on the choice of fractionation factors and underlying photosynthetic model (Eqn 2) (Flexas *et al.*, 2008; Ubierna & Farquhar, 2014). The current study initially assumed that the fractionation factors associated with CO_2 diffusion a_m, Rubisco carboxylation b, respiration e', and photorespiration f were independent of temperature. Previously, Evans & von Caemmerer (2013) validated these assumptions for the temperature response of $\Delta^{13}C$-g_m at 2% O in tobacco and subsequently measured $\Delta^{13}C$-g_m in multiple C_3 species (von Caemmerer & Evans, 2015). As will be discussed shortly, these assumptions are further analyzed to determine if they can reconcile the differences between $\Delta^{13}C$-g_m and $\Delta^{18}O$-g_m in Fig. 2.

There is less information in the literature on measurements of $\Delta^{18}O$-g_m, particularly the response of $\Delta^{18}O$-g_m to short-term changes in environmental conditions such as temperature. In the *P. bisulcatum* data presented here, at < 30°C the $\Delta^{18}O$-g_m and $\Delta^{13}C$-g_m were not significantly different; however, at ≥ 30°C the $\Delta^{13}C$-g_m was significantly higher than $\Delta^{18}O$-g_m. Previous studies have reported species variation in difference between the $\Delta^{18}O$-g_m and the $\Delta^{13}C$-g_m (Gillon & Yakir, 2000; Barbour *et al.*, 2016; Loucos *et al.*, 2017). For example, Barbour *et al.* (2016) reported a nonsignificant difference between $\Delta^{18}O$-g_m and $\Delta^{13}C$-g_m in wheat but observed 80% higher $\Delta^{18}O$-g_m than $\Delta^{13}C$-g_m in tobacco, and $\Delta^{18}O$-g_m was more than double $\Delta^{13}C$-g_m in cotton at leaf temperatures between 31.1 and 33.8°C. It remains unclear

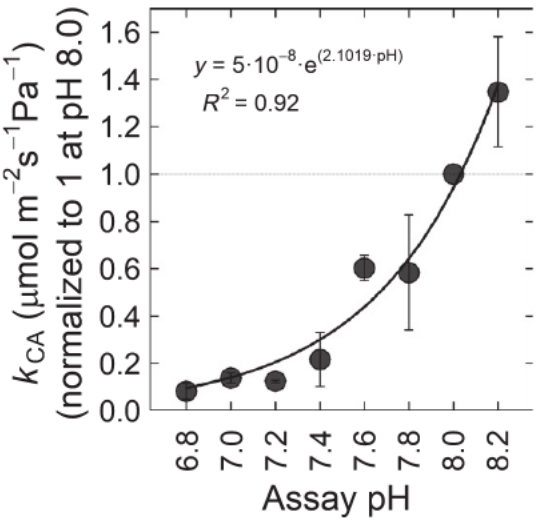

Fig. 5 The pH response of the rate constant for carbonic anhydrase hydration (k_{CA}) for *Panicum bisulcatum* measured by membrane inlet mass spectrometer at 25°C. The k_{CA} values are normalized to the measured value at pH 8.0 (dotted line). Circles are the means of three extractions from three separate plants ± SD. The solid line is the modeled pH responses using the equation shown in the graph.

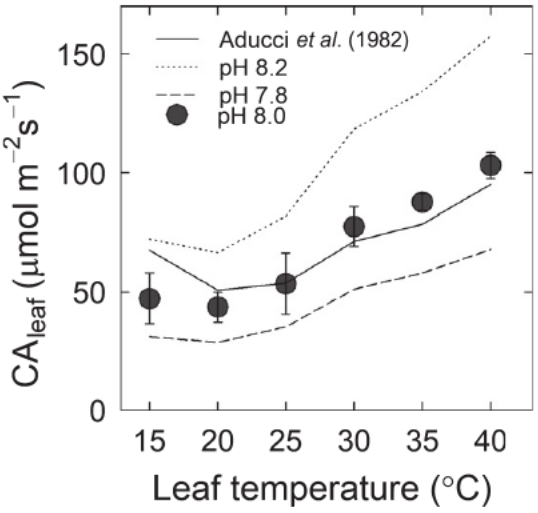

Fig. 6 Temperature response of carbonic anhydrase (CA) activity at chloroplast [CO_2] in *Panicum bisulcatum*. Chloroplast [CO_2] was calculated using $\Delta^{13}C$ method, and the k_{CA} was measured at 25°C and pH 8.0 (4.5 µmol m^{-2} s^{-1} Pa^{-1}) and modeled temperature response according to Boyd *et al.* (2015) using a modified Arrhenius model, where E_a = 40.9 kJ mol^{-1}, ΔS = 0.21 kJ mol^{-1} K^{-1}, and ΔH = 64.5 kJ mol^{-1}. Circles are the means of four biological replicates ± SD, n = 4. Modeled lines are leaf CA activity CA_{leaf} calculated using the measured pH response of k_{CA} in Fig. 5 ($k_{CA} = 5 \times 10^{-8}\, e^{2.1019 \times pH}$) with predicted temperature response of pH (solid line) and constant pH values (dashed and dotted lines).

that measurements of $\Delta^{18}O$-g_m and $\Delta^{13}C$-g_m can effectively partition g_m into its biochemical and anatomical components.

There are several assumptions needed to estimate $\Delta^{18}O$-g_m, including that: (1) the CO_2–H_2O exchange occurs at chloroplast surface; (2) there is a full isotopic equilibrium between CO_2 and H_2O at the site of exchange ($\theta = 1$); and (3) the H_2O at the site of exchange δ^{18}_{w-ce} is isotopically similar to the H_2O at the sites of evaporation δ^{18}_{w-e} (Gillon & Yakir, 2000; Barbour *et al.*, 2016). Additionally, it is generally assumed that $\Delta^{18}O$-g_m does not incorporate the resistance imposed by the chloroplast membrane and stroma, as is assumed for the $\Delta^{13}C$-g_m. Specifically, $\Delta^{18}O$-g_m provides an estimate of the internal conductance of CO_2 to the site CO_2–H_2O exchange at the chloroplast surface, whereas $\Delta^{13}C$-g_m estimates mesophyll conductance from the intercellular airspaces to the site of Rubisco fixation of CO_2 within the chloroplast stroma. Therefore, the $\Delta^{13}C$-g_m has been suggested to be *c.* 0.66 of $\Delta^{18}O$-g_m (Yakir, 1998) and can be used to separate CO_2 conductance of the chloroplast g_{ch} (i.e. chloroplast envelope and stroma) and wall g_w (i.e. cell wall, plasma membrane. and cytosol) (Gillon & Yakir, 2000). However, in addition to these potentially inherent differences between these estimates of g_m, the differences between $\Delta^{18}O$-g_m and $\Delta^{13}C$-g_m can be significantly influenced by the input parameters used in their calculation.

Assuming the calculations of $\Delta^{18}O$-g_m and $\Delta^{13}C$-g_n for *P. bisulcatum* data presented here were correctly parameterized at 25°C suggests one or more of the following: (1) the resistance to CO_2 diffusion lies entirely within the cell wall and plasma membrane; (2) the assumption for the CO_2–H_2O exchange at the chloroplast surface may be incorrect; and (3) there might be some flaws in the assumptions for the estimation of g_m in both methods (i.e. the $\Delta^{18}O$-g_m and the $\Delta^{13}C$-g_m). However, it is unlikely that the cell wall and plasma membrane provide the only resistance to CO_2 movement into the chloroplast, because the double membrane surrounding the chloroplast must impose some resistance to CO_2 diffusion (Uehlein *et al.*, 2008).

It should be noted that although $\Delta^{18}O$-g_m and $\Delta^{13}C$-g_m differed in sensitivity to temperature, both estimates increased with increasing temperature. The thermal sensitivity of CO_2 conductance in the liquid phase is thought to be limited, whereas CO_2 conductance through membranes increases exponentially with temperature (Evans & von Caemmerer, 2013). The observation of a thermal response for $\Delta^{18}O$-g_m suggests that the sites of CO_2–H_2O equilibration must lie interior to at least one membrane. However, as parameterized, the $\Delta^{18}O$-g_m measured in the current study was not as temperature sensitive as $\Delta^{13}C$-g_m. As will be discussed shortly, the difference in the temperature response of $\Delta^{18}O$-g_m and $\Delta^{13}C$-g_m may be due to errors in the assumption used in the calculations.

$\Delta^{18}O$-g_m

To our knowledge, there are no reports investigating the temperature response of $\Delta^{18}O$-g_m in C_3 species; hence, uncertainty in the assumptions associated with $\Delta^{18}O$-g_n with changing temperature remained unexplored. Therefore, we tested these assumptions with the caveat that $\Delta^{18}O$-g_m measures g_m to the chloroplast surface and that $\Delta^{13}C$-g_m estimates g_m to the site of carboxylation such that the inherent difference between $\Delta^{13}C$-g_m and $\Delta^{18}O$-g_m is primarily determined by the conductance across the chloroplast envelope and can be accounted for as $\Delta^{13}C$-$g_m \approx 0.66 \times \Delta^{18}O$-$g_m$ across temperatures (Yakir, 1998). Under this scenario, the modeled θ was significantly < 1 at ≥ 30°C. Alternatively, assuming that θ was constant across temperatures, the modeled δ^{18}_{w-e} required to minimize the difference between $\Delta^{13}C$-g_m and $\Delta^{18}O$-g_n was significantly higher at ≥ 30°C than the calculated δ^{18}_{w-e}.

The assumption that the isotopic composition between the H_2O at the site of exchange δ^{18}_{w-ce} is the same as that at the sites of evaporation δ^{18}_{w-e} depends on the spatial separation of these two locations within the leaf and the potential spatial variation of the isotopic signature of H_2O within the leaf. Alternatively, the assumption that there is a full isotopic equilibrium between CO_2 and H_2O at the site of exchange (e.g. $\theta = 1$) is primarily determined by the activity of CA. Moreover, the temperature effect on CA activity and differences between δ^{18}_{w-ce} and δ^{18}_{w-e} must also be taken into account.

Leaf temperature may affect CA activity due to temperature-mediated changes in CA catalytic properties and potentially shifts in the cytosolic/chloroplastic pH. Additionally, deactivation of CA in *S. viridis* at temperatures >25°C was reported by Boyd *et al.* (2015), suggesting that the CA activity may limit θ at higher temperatures, particularly if chloroplast [CO_2] also decreases. However, the increase of $\Delta^{13}C$-g_m with temperature suggests that chloroplast [CO_2] also increases with temperature, potentially offsetting any deactivation of CA. Furthermore, at 25°C we observed an exponential increase in CA hydration rate k_{CA} from pH 6.8 to 8.2 (Fig. 5), similar to that previously published by Berg *et al.* (2015). If pH changed with temperature, as previously reported by Aducci *et al.* (1982), who saw a 0.5 unit decrease in the cytosolic pH of maize root tip tissue with increasing temperature from 4 to 28°C, this would significantly influence not only CA activity but also potentially other reactions. Unfortunately, to our knowledge, there are no reports addressing temperature dependency of cytosolic or chloroplast pH in a photosynthetically active leaf, and to measure *in vivo* pH is technically beyond the scope of the present study.

However, modeling CA activity in response to temperature at both pH 8.2 and pH 7.8 demonstrates that a relatively small change in pH could have a significant influence on CA_{leaf}. Therefore, a potential decrease in cytosolic/chloroplastic pH with temperature may lead to a decrease in θ due to reduced CA activity. It is worth noting that CA_{leaf} in *P. bisuclatum* is low relative to other C_3 species (Gillon & Yakir, 2000). The low CA activity in *P. bisuclatum* may lower θ, particularly at high leaf temperatures, and this response might not be as pronounced in species with higher CA_{leaf}. Therefore, future studies on the temperature response of CA activity in C_3 species with diverse levels and/or anti-CA lines of tobacco, Arabidopsis, and rice are needed.

It is also possible that the isotopic signature of H_2O at the sites of evaporation δ^{18}_{w-e} as calculated with the Craig–Gordon model (Eqn 7) does not accurately represent the signature of H_2O at the site of exchange δ^{18}_{w-ce}. In C_3 plants, it has been proposed that the

site of O exchange between leaf H_2O and CO_2 is primarily located at the chloroplast surface (Yakir, 1998; Fabre *et al.*, 2007). The majority of chloroplast in the mesophyll cells in C_3 plants is appressed to the cell walls adjacent to the intercellular airspace, so it is generally assumed that δ^{18}_{w-e} is a good approximation of δ^{18}_{w-ce} (Gillon & Yakir, 2000; Barbour *et al.*, 2016). This assumes that the site of evaporation occurs near the cell walls next to the intercellular airspace in close proximity to the chloroplast. However, the site of H_2O evaporation within the leaf is not specifically known and may occur relatively far from the mesophyll cells adjacent to guard cells (Sack & Holbrook, 2006; Buckley *et al.*, 2017). Furthermore, it has been long recognized that bulk leaf H_2O is more depleted than δ^{18}_{w-e} due to the combined contribution of source H_2O and the H_2O at the sites of evaporation. Several models have been developed (e.g. the two-pool and the Péclet models) to described how the isotopic composition of bulk leaf H_2O is influenced by source H_2O and the H_2O at the sites of evaporation (Farquhar & Lloyd, 1993; Gillon & Yakir, 2000; Barbour & Farquhar, 2003; Tomás *et al.*, 2013; Barbour *et al.*, 2016; Holloway-Phillips *et al.*, 2016). However, it remains unclear what type of isotopic gradient might occur within a transpiring leaf, making it difficult to precisely parameterize the δ^{18}_{w-ce} from measurements of δ^{18}_{w-e}, particularly if the site of exchange is relatively distant from the sites of evaporation. This uncertainty is compounded by the fact that the location of O exchange between CO_2 and leaf H_2O is unknown and may differ as rates of transpiration and leaf temperature change. In fact, Barbour *et al.* (2016) demonstrated that estimates of $\Delta^{18}O$-g_m are significantly sensitive to changes in the Péclet effect. Taken together, it remains unclear how to effectively parameterize θ and the discrepancies between δ^{18}_{w-ce} and δ^{18}_{w-e} when estimating $\Delta^{18}O$-g_m. However, it appears clear that the assumptions used at 25°C likely do not hold true for higher temperatures.

Conclusion

We have estimated temperature responses of $\Delta^{13}C$-g_m and the $\Delta^{18}Og_m$ using coupled leaf gas exchange and isoflux measurements of CO_2 and transpired H_2O in C_3 *P. bisulcatum*. Our observations are unable to partition g_m into its components (i.e. g_w and g_{ch}) and their temperature dependency because of uncertainties in the temperature response of several input parameters. However, the data presented here suggest that the highest uncertainties are associated with the assumptions made in calculating $\Delta^{18}O$-g_m (e.g. θ and $\delta^{18}_{w-e} = \delta^{18}_{w-ce}$). Future work to obtain precise information on the temperature dependency of cytosolic and chloroplastic pH could better enable partitioning of g_m into its components and their responses to environmental changes using combined measurements of $\Delta^{13}C$-g_m and the $\Delta^{18}Og_m$.

Acknowledgements

This research was supported by the Office of Science (BER), US Department of Energy, Grant no. DE-SC0014395. The authors thank Drs N. Ubierna, R. Giuliani, and P. Z. Ellsworth for their timely and valuable comments for the study. We are grateful to Charles A. Cody for plant growth management. We would also like to thank Dr Margaret Barbour and two anonymous referees for their helpful feeding back during the review process.

Author contributions

BVS and ABC designed the experiment. BVS performed the measurements. BVS and ABC analyzed the data and wrote the manuscript.

ORCID

Asaph B. Cousins https://orcid.org/0000-0003-2424-714X
Balasaheb V. Sonawane https://orcid.org/0000-0001-6539-5179

References

Aducci P, Federico R, Carpinelli G, Podo F. 1982. Temperature dependence of intracellular pH in higher plant cells. *Planta* **156**: 579–582.

Badger MR, Price GD. 1989. Carbonic anhydrase activity associated with the *Cyanobacterium Synechococcus* PCC7942. *Plant Physiology* **89**: 51–60.

Barbour MM, Evans JR, Simonin KA, von Caemmerer S. 2016. Online CO_2 and H_2O oxygen isotope fractionation allows estimation of mesophyll conductance in C_4 plants, and reveals that mesophyll conductance decreases as leaves age in both C_4 and C_3 plants. *New Phytologist* **210**: 875–889.

Barbour MM, Farquhar GD. 2003. Do pathways of water movement and leaf anatomical dimensions allow development of gradients in $H_2{}^{18}O$ between veins and the sites of evaporation within leaves? *Plant, Cell & Environment* **27**: 107–121.

Bates D, Martin M, Bolker B, Walker S. 2015. Fitting linear mixed-effects models using LME4. *Journal of Statistical Software* **67**: 1–48.

Berg JM, Tymoczko JL, Stryer L, Berg JM, Tymoczko JL, Stryer L. 2015. *Biochemistry*. New York, NY, USA: W. H. Freeman.

Bottinga Y, Craig H. 1968. Oxygen isotope fractionation between CO_2 and water, and the isotopic composition of marine atmospheric CO_2. *Earth and Planetary Science Letters* **5**: 285–295.

Boyd RA, Gandin A, Cousins AB. 2015. Temperature responses of C_4 photosynthesis: biochemical analysis of Rubisco, phosphoenolpyruvate carboxylase, and carbonic anhydrase in *Setaria viridis*. *Plant Physiology* **169**: 1850–1861.

Buckley TN, John GP, Scoffoni C, Sack L. 2017. The sites of evaporation within leaves. *Plant Physiology* **173**: 1763–1782.

von Caemmerer S, Evans JR. 2015. Temperature responses of mesophyll conductance differ greatly between species. *Plant, Cell & Environment* **38**: 629–637.

Cernusak LA, Farquhar GD, Wong SC, Stuart-Williams H. 2004. Measurement and interpretation of the oxygen isotope composition of carbon dioxide respired by leaves in the dark. *Plant Physiology* **136**: 3350–3363.

Cousins AB, Badger MR, von Caemmerer S. 2008. C_4 photosynthetic isotope exchange in NAD-ME- and NADP-ME-type grasses. *Journal of Experimental Botany* **59**: 1695–1703.

Douthe C, Dreyer E, Epron D, Warren CR. 2011. Mesophyll conductance to CO_2, assessed from online TDL-AS records of $^{13}CO_2$ discrimination, displays small but significant short-term responses to CO_2 and irradiance in *Eucalyptus* seedlings. *Journal of Experimental Botany* **62**: 5335–5346.

Evans JR, von Caemmerer S, Setchell B, Hudson G. 1994. The relationship between CO_2 transfer conductance and leaf anatomy in transgenic tobacco with a reduced content of Rubisco. *Functional Plant Biology* **21**: 475–495.

Evans JR, von Caemmerer S. 1996. Carbon dioxide diffusion inside leaves. *Plant Physiology* **110**: 339–346.

Evans JR, Kaldenhoff R, Genty B, Terashima I. 2009. Resistances along the CO_2 diffusion pathway inside leaves. *Journal of Experimental Botany* **60**: 2235–2248.

Evans JR, Sharkey T, Berry J, Farquhar G. 1986. Carbon isotope discrimination measured concurrently with gas exchange to investigate CO_2 diffusion in leaves of higher plants. *Functional Plant Biology* **13**: 281–292.

Evans JR, von Caemmerer S. 2013. Temperature response of carbon isotope discrimination and mesophyll conductance in tobacco. *Plant, Cell & Environment* **36**: 745–756.

Fabre N, Reiter IM, Becuwe-Linka N, Genty B, Rumeau D. 2007. Characterization and expression analysis of genes encoding α and β carbonic anhydrases in *Arabidopsis*. *Plant, Cell & Environment* **30**: 617–629.

Farquhar GD, Cernusak LA. 2012. Ternary effects on the gas exchange of isotopologues of carbon dioxide. *Plant, Cell & Environment* **35**: 1221–1231.

Farquhar GD, Hubick KT, Condon AG, Richards RA. 1989. Carbon isotope fractionation and plant water-use efficiency. In: Rundel PW, Ehleringer JE, NAgy KA, eds. *Stable isotopes in ecological research*. New York, NY, USA: Springer, 21–40.

Farquhar GD, Lloyd J. 1993. 5 – Carbon and oxygen isotope effects in the exchange of carbon dioxide between terrestrial plants and the atmosphere. In: Ehleringer JR, Hall AE, Farquhar GD, eds. *Stable isotopes and plant carbon–water relations*. San Diego, CA, USA: Academic Press, 47–70.

Flexas J, Diaz-Espejo A, Galmés J, Kaldenhoff R, Medrano H, Ribas-Carbo M. 2007. Rapid variations of mesophyll conductance in response to changes in CO_2 concentration around leaves. *Plant, Cell & Environment* **30**: 1284–1298.

Flexas J, Ribas-Carbó M, Diaz-Espejo A, Galmés J, Medrano H. 2008. Mesophyll conductance to CO_2: current knowledge and future prospects. *Plant, Cell & Environment* **31**: 602–621.

Gillon JS, Yakir D. 2000. Internal conductance to CO_2 diffusion and C ^{18}OO discrimination in C_3 leaves. *Plant Physiology* **123**: 201–214.

Harned HS, Bonner FT. 1945. The first ionization of carbonic acid in aqueous solutions of sodium chloride. *Journal of the American Chemical Society* **67**: 1026–1031.

Hatch MD, Burnell JN. 1990. Carbonic anhydrase activity in leaves and its role in the first step of C_4 photosynthesis. *Plant Physiology* **93**: 825–828.

Holloway-Phillips M, Cernusak LA, Barbour M, Song X, Cheesman A, Munksgaard N, Stuart-Williams H, Farquhar GD. 2016. Leaf vein fraction influences the Péclet effect and ^{18}O enrichment in leaf water. *Plant, Cell & Environment* **39**: 2414–2427.

Jenkins CLD. 1989. Effects of the phosphoenolpyruvate carboxylase inhibitor 3,3-dichloro-2-(dihydroxyphosphinoylmethyl)propenoate on photosynthesis: C_4 selectivity and studies on C_4 photosynthesis. *Plant Physiology* **89**: 1231–1237.

Kolbe AR, Cousins AB. 2018. Mesophyll conductance in *Zea mays* responds transiently to CO_2 availability: implications for transpiration efficiency in C_4 crops. *New Phytologist* **217**: 1463–1474.

Loucos KE, Simonin KA, Barbour MM. 2017. Leaf hydraulic conductance and mesophyll conductance are not closely related within a single species. *Plant, Cell & Environment* **40**: 203–215.

Niinemets U, Cescatti A, Rodeghiero M, Tosens T. 2006. Complex adjustments of photosynthetic potentials and internal diffusion conductance to current and previous light availabilities and leaf age in Mediterranean evergreen species *Quercus ilex*. *Plant, Cell & Environment* **29**: 1159–1178.

O'Leary MH, Madhavan S, Paneth P. 1992. Physical and chemical basis of carbon isotope fractionation in plants. *Plant, Cell & Environment* **15**: 1099–1104.

R Core Team. 2017. *R (3.4.3): a language and environment for statistical computing*. Vienna, Austria: R Foundation for Statistical Computing.

Sack L, Holbrook NM. 2006. Leaf hydraulics. *Annual Review of Plant Biology* **57**: 361–381.

Sander R. 2015. Compilation of Henry's law constants (version 4.0) for water as solvent. *Atmospheric Chemistry and Physics* **15**: 4399–4981.

Silverman DN. 1982. Carbonic anhydrase: oxygen-18 exchange catalyzed by an enzyme with rate-contributing Proton-transfer steps. *Methods in Enzymology*. **87**: 732–752.

Simonin KA, Roddy AB, Link P, Apodaca R, Tu KP, Hu J, Dawson TE, Barbour MM. 2013. Isotopic composition of transpiration and rates of change in leaf water isotopologue storage in response to environmental variables. *Plant, Cell & Environment* **36**: 2190–2206.

Sharwood RE, Ghannoum O, Kapralov MV, Gunn LH, Whitney SM. 2016. Temperature responses of Rubisco from Paniceae grasses provide opportunities for improving C_3 photosynthesis. *Nature Plants* **2**: 16186.

Tazoe Y, Von Caemmerer S, Estavillo GM, Evans JR. 2011. Using tunable diode laser spectroscopy to measure carbon isotope discrimination and mesophyll conductance to CO_2 diffusion dynamically at different CO_2 concentrations. *Plant, Cell & Environment* **34**: 580–591.

Tcherkez G, Farquhar GD. 2005. Carbon isotope effect predictions for enzymes involved in the primary carbon metabolism of plant leaves. *Functional Plant Biology* **32**: 277–291.

Tomás M, Flexas J, Copolovici L, Galmés J, Hallik L, Medrano H, Ribas-Carbó M, Tosens T, Vislap V, Niinemets U. 2013. Importance of leaf anatomy in determining mesophyll diffusion conductance to CO_2 across species: quantitative limitations and scaling up by models. *Journal of Experimental Botany* **64**: 2269–2281.

Ubierna N, Farquhar GD. 2014. Advances in measurements and models of photosynthetic carbon isotope discrimination in C_3 plants. *Plant, Cell & Environment* **37**: 1494–1498.

Ubierna N, Gandin A, Boyd RA, Cousins AB. 2017. Temperature response of mesophyll conductance in three C_4 species calculated with two methods: ^{18}O discrimination and *in vitro* V_{pmax}. *New Phytologist* **214**: 66–80.

Ubierna N, Sun W, Kramer DM, Cousins AB. 2013. The efficiency of C4 photosynthesis under low light conditions in *Zea mays, Miscanthusx giganteus* and *Flaveria bidentis*. *Plant, Cell & Environment* **36**: 365–381.

Uehlein N, Otto B, Hanson DT, Fischer M, McDowell N, Kaldenhoff R. 2008. Function of *Nicotiana tabacum* aquaporins as chloroplast gas pores challenges the concept of membrane CO_2 permeability. *Plant Cell* **20**: 648–657.

Warren CR. 2008. Stand aside stomata, another actor deserves centre stage: the forgotten role of the internal conductance to CO_2 transfer. *Journal of Experimental Botany* **59**: 1475–1487.

Yakir D. 1998. Oxygen-18 of leaf water: a crossroad for plant-associated isotopic signals. In: Griffiths H, ed. *Stable isotopes: integration of biological, ecological and geochemical processes*. Oxford, UK: BIOS Scientific Publishers, 147–168.

Supporting Information

Additional Supporting Information may be found online in the Supporting Information section at the end of the article:

Fig. S1 Sensitivity of Picarro (L2130-i) for δ^{18}O measurements to the water vapor concentration.

Fig. S2 Temperature response of transpiration rates.

Fig. S3 Corrections of δ^{18}O of transpired water (δ^{18}_{w-E}) by accounting δ^{18}O offset of Picarro (L2130-i).

Methods S1 Calculations for CO_2 mesophyll conductance from Δ^{18}O (Δ^{18}O-g_m).

Table S1 Parameters and units or values for calculation of g_m with the Δ^{13}C-g_m method.

Table S2 Parameters and units or values for calculation of g_m with the Δ^{18}O-g_m method.

Table S3 Summary of temperature response for gas exchange, isoflux and mesophyll conductance (calculated under standard assumptions) for the youngest fully expanded leaf of *Panicum bisulcatum*.

Please note: Wiley Blackwell are not responsible for the content or functionality of any Supporting Information supplied by the authors. Any queries (other than missing material) should be directed to the *New Phytologist* Central Office.